

RESEARCH ARTICLE

Synthesis of Ag-Fe₂O₃ nanoparticles with Anti-bacterial and anti-fungal impacts on dental microbia

Kamyar Nasiri*

Department of dentistry, Islamic Azad University, Tehran, Iran

ARTICLE INFO

Article History:

Received 03 Feb 2023

Accepted 18 Apr 2023

Published 01 May 2023

Keywords:

Ag-Fe₂O₃ nanoparticles
Streptococcus mutans
Streptococcus mutans
dental microbial

ABSTRACT

The arrangement of silver doped iron oxide nanoparticles (Ag-Fe₂O₃ NPs) through the exploitation of *Prosopis fratta* leaf extract was successfully performed in this work, which was proceeded by configuring the produced NPs by the outcomes of Powder X-ray Diffraction (PXRD), Field Energy Scanning Electron Microscopy (FESEM), Energy-Dispersive X-ray (EDX), Raman, Fourier Transform Infrared (FT-IR), and Vibrating-Sample Magnetometer (VSM) procedures. Apparently, the observed spherical particulates contained a size of 50-60 nm, while exhibiting antimicrobial performances towards *Streptococcus mutans bacteria* and *Candida albicans fungi*. They also seemed to possess potential antibacterial and anti-fungi properties at the volumes of 10 and 75 µg/mL, respectively, and thus, a viable proposal can be made regarding our synthesized product as a suitable option for dental and oral implementations. In addition, this biosynthesis method can be a suitable option for the synthesis of nanoparticles due to advantages such as cost-effectiveness, environmental friendliness, and no use of chemical solvents.

How to cite this article

Nasiri K. Synthesis of Ag-Fe₂O₃ nanoparticles with Anti-bacterial and anti-fungal impacts on dental microbia. *Nanomed Res J*, 2023; 8(3): 283-289. DOI: 10.22034/nmrj.2023.03.007

INTRODUCTION

The presented substantial platform by nanotechnology for altering the physicochemical features of countless materials, under the aim of generating effectual antimicrobials, Nanomaterials (NM), can offer strategical benefits in the form of active antibacterial groups with exceedingly large surface areas in proportion to their sizes. The capability of nano sized particles in causing high rates of activity despite the usage of small doses has been well proved, which confirms the capacity of Nanomaterials in supplying an alternative for antibiotics in the course of controlling bacterial infections [1]. Metal oxides such as ZnO, TiO₂, Fe₂O₃ and CuO nanoparticles are included among the metal oxides with a strong potential for acting as antibacterial products. For instance, many researchers invested their interest in Fe₂O₃ nanoparticles that contain a band gap of ~2.2 eV for bacterial inhibition, which is attributable to its visible light absorption qualities (~564 nm),

distinctive magnetic features, and biocompatibility [2-5]. The interaction of released iron oxide nanoparticle into the environment with air, water, and soil usually induces alterations in the surface quantities of particles and leads to particle accumulation or modifications in particle charge and other surface features. Different surface adjustments were attempted for discovering the right designs of these non-biodegradable nanoparticles with superior biocompatibility [6-8]. The approach of surface modification is performed under the objective of enhancing the surface characteristics of iron oxide nanoparticles. This technic can inhibit the occurrence of aggregation, as well as upgrade the compatibility of iron oxide nanoparticles with biological surroundings and their stability in suspensions [8-10]. The fundamental stance of silver nanoparticles in the progress of novel antimicrobial substances against certain pathogenic microorganisms is undeniable. Additionally, the smaller size of these nanoparticles is quite effectual in enhancing the

* Corresponding Author Email: kamyar.nasiri.dds@gmail.com

antibacterial performance through the lysis of bacterial cell wall [2, 11-14]. Apparently, although not many papers were published on the synthesis of Ag/Fe₂O₃ nanoparticles [15], there are reports on the synthesis of various heteromers of Ag/Fe₂O₃ nanoparticles and their bactericidal performances [16], the synthesis of Ag/Fe₂O₃ nanoparticles by glucose, and most recently [17] on the synthesis of Ag/Fe₂O₃ nanoparticles through the exertion of green *Adathoda vasica* leaf extract to achieve antibacterial, antifungal and anticancer features.

Numerous research results confirmed the upgraded antimicrobial functionality of Ag/Fe₂O₃ nanoparticles in contrast to the solitary case of Fe₂O₃ nanoparticles [15, 17]. Their observations pointed out the significance of released Ag⁺ ions from Ag/Fe₂O₃ nanoparticles in the process of antibacterial activities [12, 15, 17]. There is no doubt in the superior effectiveness of Ag/Fe₂O₃ nanoparticles than that of solitary Ag NP in the cases of pathogens similar to bacteria, as well as fungi as multi drug resistant pathogens, which is attributable to the manageable release of Ag⁺ ions [11]. Our work is based on the synthesis of Fe₂O₃ nanoparticles through a Hydrothermal approach and proceeded by the arrangement of Ag doping Fe₂O₃ through a photodeposition route [18]. We also assayed the constructional configurations and antibacterial performances of Fe₂O₃ and Ag/Fe₂O₃ nanoparticles towards *shigella dysenteriae* bacteria.

Performing the biosynthesis of materials through plant extracts proved to be uncomplicated, methodical, cost-efficient, and pertinent, which can serve as fitting substitutes for conventional preparation routes of extending the manufacturing of nanoparticles [19]. The biomolecules of plants, similar to carbohydrates, proteins, and coenzymes, can efficiently facilitate the reduction of metal salts into nanoparticles while preserving their stabilization [19]. Considering these facts, our work proceeded under the objective of synthesizing Ag-Fe₂O₃ NPs through the exploitation of leaf extract of *Prosopis farcta*, which was continued by assessing the antimicrobial performance of our product towards *Streptococcus mutans* bacteria and *Candida albicans* fungi.

MATERIALS AND METHOD

Synthesis of Ag-Fe₂O₃ NPs

As the first step, the impure substances of *Prosopis farcta* leaves were dispatched by being washed with DI water to be dried in the course

of 2 days at ambient temperature. Subsequent to weighing out 10 g of the leaves and appending 100 mL of DI water, the mixture was heated for 30 min at 90 °C, which was then filtered to cleanse out the broth and collect the resultant extract for the upcoming experiments. The synthesizing process of Ag-Fe₂O₃ required the consistent insertion of a fitting aqueous solution of extracted *Prosopis farcta* to the mixture of 0.1 M of FeCl₃ and 0.025 M of Ag (NO₃) within an Erlenmeyer flask under stirring conditions by a magnetic stirrer at 75 °C for 2 h. Succeeding to tuning the pH of solution through the exertion of NaOH (1M, Merck, pH=11), the prepared mixture was heated in oven at 90 °C for 12 h. The prepared precipitate by drying the resultant was calcinated in a furnace at 400 °C for 2 h to fabricate the brown powder of Ag-Fe₂O₃ NPs.

Characterization

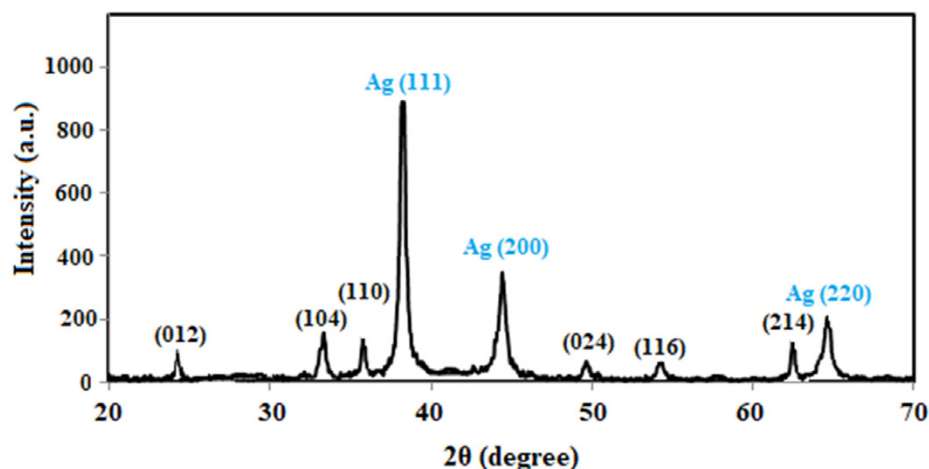
The characteristics of Ag-Fe₂O₃ NPs was determined through X-ray powder diffractometer (XRD) and scanning electron microscope (SEM). The type of exerted XRD was PANalytical X'Pert PRO MPD system X-Ray Diffractometer, which implicated the 2θ values in a scale of 20° to 80° along with the Cu Kα radiation source (λ=1.54060) that functioned at 40 kV and 25 mA. Furthermore, the employed type of SEM was MIRA3 TESCAN.

Assessment of the Inhibitory Activity of Ag-Fe₂O₃ NPs

In the following, we performed a well-diffusion trial to collect data on the inhibitory performance of Ag-Fe₂O₃ NPs towards *Streptococcus mutans* bacteria. For this purpose, the streaking technic was exerted to inoculate the experimental bacteria into the sterile Petri plates that were composed of 20 mL of Mueller-Hinton. As the wells were made ready by the employment of sterile corn borer (6 mm), the appending of 200 μL of NPs at the volumes of 1, 4, 8, 10 mg/mL was required to continue the process. We stored the inoculated plates in a refrigerator for 45 min to complete the adequate diffusion of NPs and thus, performed the bacteria assay through an incubation procedure at 37 °C for 24 h. Lastly, the surrounding inhibition zone of every well was determined.

Assessment of Antifungal Activity of Ag-Fe₂O₃ NPs

The antifungal functionality of our product was configured through the outcomes of agar well diffusion technic. Under this objective, we exerted week-old fungal cultures grown on potato

Fig. 1. PXRD spectrum of Ag-Fe₂O₃ NPs

dextrose medium to assay the antifungal potential of designated NPs. The inoculation of aliquots of 0.02 mL inocula from every fungal pathogen was done within 20 mL of molten Sabouraud dextrose agar medium in culture tubes, which were subsequently homogenized among hands to be inserted into 90 mm Petri plates. As the following step, we provided the solidification of culture plates in laminar airflow chamber to prepare the wells on the agar plate by a 5 mm standard corn borer. The exerted culture tubes, culture plates, and laminar airflow were procured from Thermo Fischer Scientific, New Delhi, India. A diverse range of NPs concentration (25, 50, and 75 μ L of 0.10 mg/mL NPs) was appended to respective wells, while Hexahit 0.1 mg/mL (20 μ L/disc) was implicated as the standard (positive control). We examined the impact of our product on fungal pathogens and conducted a comparison between its results and that of the standard. Thereafter, we sealed the plates to perform an incubation at 25 ± 2 °C for the duration of 2 days and ultimately, the antifungal functionality was required to be determined through the measurement of inhibition zone through the standard scale.

RESULTS AND DISCUSSION

PXRD analysis

Fig. 1 exhibits the powder x-ray diffraction spectrum of Ag-Fe₂O₃ NPs, which displays the diffraction pattern of Fe₂O₃ with peaks in the 2θ positions of 25.21, 34.12, 35.58, 49.51, 53.71, 58.86, and 61.28° that were associated with the (021), (104), (110), (024), (116), (018), and (214) planes.

In coordination to this figure, certain other peaks were discerned throughout the 2θ position of 38.1, 43.2, 65.4, and 72.1° as the signs of silver atoms existence in the crystalline construction of doped nanoparticles. In consonance with the diffraction peak at $2\theta = 35.58^\circ$, we determined the crystalline particle size of Fe₂O₃ through the Debye-Scherrer's equation to be 41.59 nm for Ag-Fe₂O₃ NPs.

FESEM and EDX analysis

The data of SEM images (Fig. 2A) aided the configuring process of synthesized Ag-Fe₂O₃ NPs in term of morphology and size of particles, which exhibited spherical doped nanoparticles in the size of 50-60 nm. Similar to PXRD outcomes, Fig. 2A proves the doping impacts of silver into the iron oxide structure on causing a decrease in particle size. The EDX data in Fig. 2B provides an evident proof for the appearance of doped silver throughout the nanoparticles.

VSM analysis

The analytical data of VSM helped in configuring the magnetic features of synthesized Ag-Fe₂O₃ NPs (Fig. 3) and as it is observable, the value of saturation magnetization was 0.16 emu/g, while the same parameter (M_s) for the Fe₂O₃ of our previous study was reported to be 1.8 emu/g [20]. These outcomes imply the effect of existing silver in nanoparticles construction on reducing the rate of saturation magnetization in samples, which is probably attributable to the nature of paramagnetic substances as a hard magnetic material. A direct connection among the M_s content of these NPs

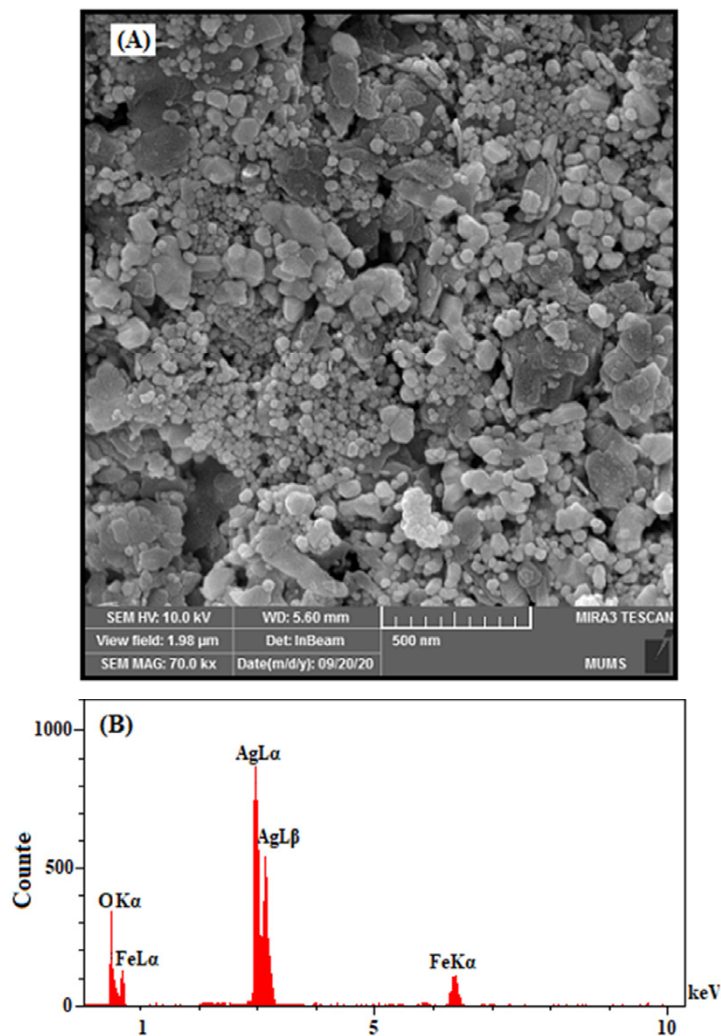


Fig. 2. (A) FESEM and (B) EDX spectra of Ag-Fe₂O₃ NPs

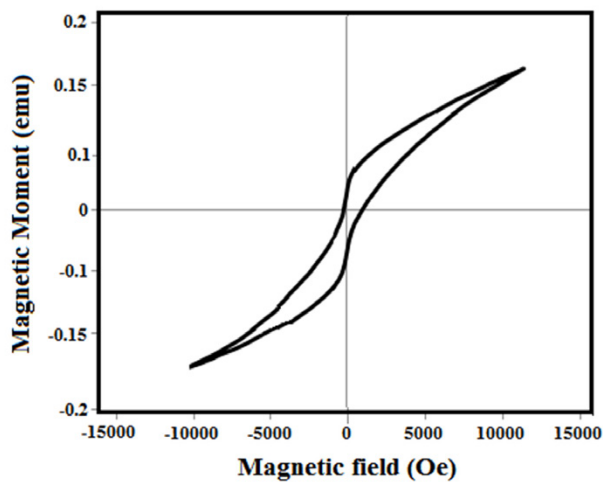
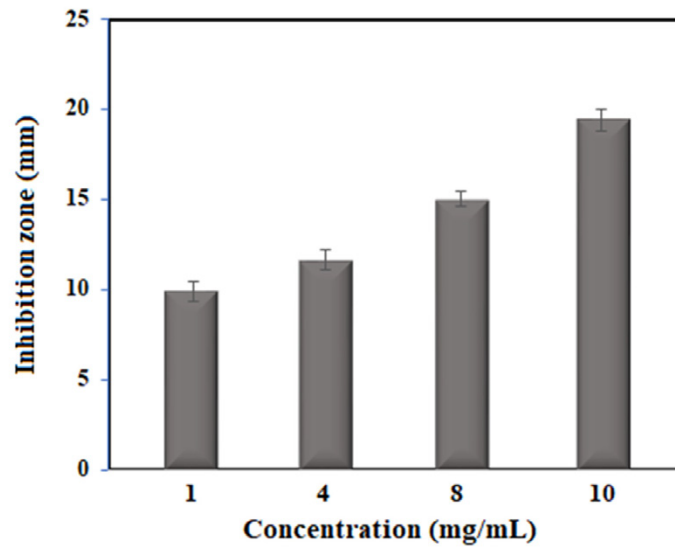


Fig. 3. VSM spectra of Ag-Fe₂O₃ NPs

Fig. 4. Antimicrobial activity of the synthesized Ag-Fe₂O₃ NPsTable 1. Antifungal activity of Ag-Fe₂O₃ NPs

	Activity against the fungi (mm)			
	Control (20 μ L)	Ag-Fe ₂ O ₃ (25 μ L)	Ag-Fe ₂ O ₃ (50 μ L)	Ag-Fe ₂ O ₃ (75 μ L)
<i>Candida albicans</i>	25	10	12	16

and their particle size and shape anisotropy were discovered by the survey of Bepari and his coworkers on the magnetic features of Fe₂O₃ NPs [20].

Anti-bacterial assay

Fig. 4 displays the data of well diffusion procedure, which was exerted to assess the antibacterial efficacy of Ag-Fe₂O₃ NPs towards *Streptococcus mutans*. The maximal dosage of Ag/Fe₂O₃ (10 g/mL) exhibited a high level of inhibitory performance on *Streptococcus mutans* along with the inhibition zones of 19 \pm 0.45 mm (Fig. 4). A related assessment proved the superior antimicrobial impacts of silver particles on hazardous Gram-positive or Gram-negative bacteria [21]. Similarly, some recent researchers studied the antibacterial performance of Ag-Fe₂O₃ and approved its suitability on Gram-negative and Gram-positive bacteria as well [22-24]. The antibacterial functionality of Ag-Fe₂O₃ towards bacteria is attributable to its capabilities in damaging the cell walls, disrupting constructional proteins, inactivating enzymes, preventing electron

transport chains, injuring nucleic acids (DNA), and facilitating the induction of oxidative stress through reactive oxygen species (ROS) [10, 25-27]. In this regard, the emergence of Ag-Fe₂O₃ as a practicable antibacterial treatment choice can be quite advantageous in medicinal fields as well.

Anti-fungi assay

As a role model sample, *Candida albicans* fungi was exerted to assess the antifungal performance of Ag-Fe₂O₃ NPs. It is considerable that a very limited number of reports are available on the application of iron oxide NPs in the form of antifungal materials towards these two fungi. The work of Nazanin implicated the exploitation of spherical iron oxide NPs in the size of 30–40 nm for the case of fungal infection by *Candida* species, which resulted in exhibiting the antifungal capacity of NP against pathogenic *Candida* spp. [28]. Moreover, Nehra et al. [29] reported their successful results on illustrating the antifungal functionality of chitosan-coated iron oxide NPs in opposition to *A. niger* and four different organisms. In a close correspondence to our discoveries, the mean diameter of inhibition

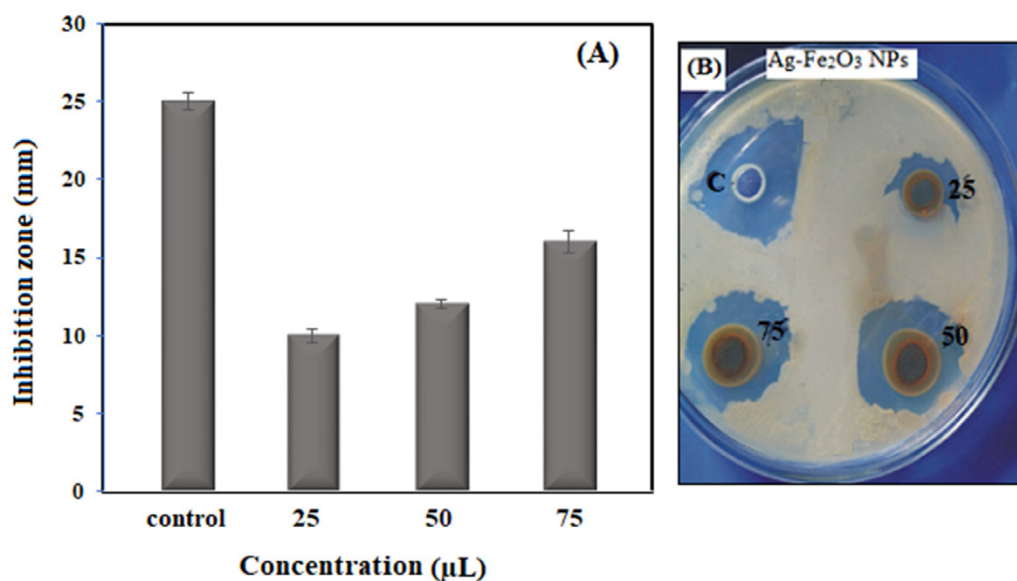


Fig. 5. Antifungal activity of Ag-Fe₂O₃ NPs against *Candida albicans*

zone of the prepared chitosan-coated NPs contained a scale of 14.5–18.5 mm.

The activities of Ag-Fe₂O₃ NPs are outlined in Table 1 and rendered in Fig. 5. The large surface-to-volume ratio of NP can facilitate their strong adherence to the cell surfaces of fungus, while their small sizes can provide a direct penetration into the cells and result in injuring the cell walls. Ag-Fe₂O₃ NPs are able to inactivate fungus by utilizing the head on interactions of NPs with cell surfaces, which influences the permeability of membranes upon the entry of NPs to induce oxidative stress in fungus cells. This process ultimately prevents the growth of cells and gradually results in cell annihilation [30].

In conformity to literature, there are the probabilities of membrane injury through the straight or electrostatic interaction of Ag-Fe₂O₃ NPs with cell surfaces, NPs cellular internalization, and the generation of active oxygen species similar to H₂O₂ within cells by metal oxides [31]. Furthermore, Fig. 5B exhibits the noticeable antifungal performance of Ag-Fe₂O₃ NPs towards *Candida albicans*. There is a firm belief among the authors on the robust interaction of Ag-Fe₂O₃ NPs with the cell surface of *Candida albicans*.

CONCLUSIONS

This paper was set out to exploit the extracted product of *Prosopis farcta* leaf to conduct an

uncomplicated, quick, and effective synthesizing technic to fabricate Ag-Fe₂O₃ NPs. The configuration of our products qualities required the outcomes of certain analyses similar to PXRD, Raman, and FESEM and accordingly, the particle sizes were reported to be 50-60 nm for Ag-Fe₂O₃ NPs whilst observed in a spherical form. The data of hysteresis loop appointed the saturation magnetization (Ms) of Ag-Fe₂O₃ NPs to be 0.17 emu/g. We also assayed the capability of our product in exhibiting anti-bacterial effects on *Streptococcus mutans* and anti-fungi in opposition to *Candida albicans* and the attained data approved our proposal of these synthesized NPs with potential applicability throughout the fields of oral and dental health.

CONFLICT OF INTEREST

There is no conflict of interest

REFERENCES

1. Rabiee, N., et al., Silver and gold nanoparticles for antimicrobial purposes against multi-drug resistance bacteria. *Materials*, 2022. 15(5): p. 1799. <https://doi.org/10.3390/ma15051799>
2. Kouhbanani, M.A.J., et al., Green synthesis of iron oxide nanoparticles using *Artemisia vulgaris* leaf extract and their application as a heterogeneous Fenton-like catalyst for the degradation of methyl orange. *Materials Research Express*, 2018. 5(11): p. 115013. <https://doi.org/10.1088/2053-1591/aadde8>
3. Long, M., et al., Fe₂O₃ nanoparticles anchored on 2D kaolinite with enhanced antibacterial activity. *Chemical*

- Communications, 2017. 53(46): p. 6255-6258. <https://doi.org/10.1039/C7CC02905E>
4. Miri, A., S. Akbarpour Birjandi, and M. Sarani, Survey of cytotoxic and UV protection effects of biosynthesized cerium oxide nanoparticles. *Journal of Biochemical and Molecular Toxicology*, 2020. 34(6): p. e22475. <https://doi.org/10.1002/jbt.22475>
 5. Miri, A. and M. Sarani, Biosynthesis and cytotoxic study of synthesized zinc oxide nanoparticles using *Salvadora persica*. *BioNanoScience*, 2019. 9(1): p. 164-171. <https://doi.org/10.1007/s12668-018-0579-3>
 6. Abdollahi, S., et al., Adverse Effects of some of the Most Widely used Metal Nanoparticles on the Reproductive System. *Journal of Infertility and Reproductive Biology*, 2020. 8(3): p. 22-32. [https://doi.org/10.47277/JIRB/8\(3\)/22](https://doi.org/10.47277/JIRB/8(3)/22)
 7. Elsaesser, A. and C.V. Howard, Toxicology of nanoparticles. *Advanced drug delivery reviews*, 2012. 64(2): p. 129-137. <https://doi.org/10.1016/j.addr.2011.09.001>
 8. Kouhbanani, M.A.J., et al., One-step green synthesis and characterization of iron oxide nanoparticles using aqueous leaf extract of *Teucrium polium* and their catalytic application in dye degradation. *Advances in Natural Sciences: Nanoscience and Nanotechnology*, 2019. 10(1): p. 015007. <https://doi.org/10.1088/2043-6254/aafe74>
 9. Arakha, M., et al., Antimicrobial activity of iron oxide nanoparticle upon modulation of nanoparticle-bacteria interface. *Scientific reports*, 2015. 5(1): p. 14813. <https://doi.org/10.1038/srep14813>
 10. Mosleh-Shirazi, S., et al., Biosynthesis, simulation, and characterization of Ag/AgFeO₂ core-shell nanocomposites for antimicrobial applications. *Applied Physics A*, 2021. 127: p. 1-8. <https://doi.org/10.1007/s00339-021-05005-7>
 11. Kouhbanani, M.A.J., et al., Green synthesis and characterization of spherical structure silver nanoparticles using wheatgrass extract. *Journal of Environmental Treatment Techniques*, 2019. 7(1): p. 142-149.
 12. Kouhbanani, M.A.J., et al., Green synthesis of spherical silver nanoparticles using *Ducrosia anethifolia* aqueous extract and its antibacterial activity. *Journal of Environmental Treatment Techniques*, 2019. 7(3): p. 461-466.
 13. Miri, A. and M. Sarani, Silver nanoparticles: cytotoxic and apoptotic activity on HT-29 and A549 cell lines. *Journal of New Developments in Chemistry*, 2018. 1(4): p. 1. <https://doi.org/10.14302/issn.2377-2549.jndc-18-2116>
 14. Patra, J.K. and K.-H. Baek, Antibacterial activity and synergistic antibacterial potential of biosynthesized silver nanoparticles against foodborne pathogenic bacteria along with its anticandidal and antioxidant effects. *Frontiers in microbiology*, 2017. 8: p. 167. <https://doi.org/10.3389/fmicb.2017.00167>
 15. Chen, Y., N. Gao, and J. Jiang, Surface matters: enhanced bactericidal property of core-shell Ag-Fe₂O₃ nanostructures to their heteromer counterparts from one-pot synthesis. *Small (Weinheim an der Bergstrasse, Germany)*, 2013. 9(19): p. 3242-3246. <https://doi.org/10.1002/sml.201300543>
 16. Kaloti, M., A. Kumar, and N.K. Navani, Synthesis of glucose-mediated Ag-γ-Fe₂O₃ multifunctional nanocomposites in aqueous medium—a kinetic analysis of their catalytic activity for 4-nitrophenol reduction. *Green Chemistry*, 2015. 17(10): p. 4786-4799. <https://doi.org/10.1039/C5GC00941C>
 17. Kulkarni, S., et al., Green synthesized multifunctional Ag@Fe₂O₃ nanocomposites for effective antibacterial, antifungal and anticancer properties. *New Journal of Chemistry*, 2017. 41(17): p. 9513-9520. <https://doi.org/10.1039/C7NJ01849E>
 18. Alkaim, A.F., et al., Synthesis, characterization, and photocatalytic activity of sonochemical/hydration-dehydration prepared ZnO rod-like architecture nano/microstructures assisted by a biotemplate. *Environmental technology*, 2017. 38(17): p. 2119-2129. <https://doi.org/10.1080/09593330.2016.1246615>
 19. Miri, A. and M. Sarani, Biological studies of synthesized silver nanoparticles using *Prosopis farcta*. *Molecular biology reports*, 2018. 45: p. 1621-1626. <https://doi.org/10.1007/s11033-018-4299-0>
 20. Khatami, M., et al., Green synthesis of amorphous iron oxide nanoparticles and their antimicrobial activity against *Klebsiella pneumoniae*, *Pseudomonas aeruginosa* and *Escherichia coli*. *Iran J Biotechnol*, 2019. 10: p. 33-39.
 21. Hashem, A.H., et al., Synthesis of chitosan-based gold nanoparticles: Antimicrobial and wound-healing activities. *Polymers*, 2022. 14(11): p. 2293. <https://doi.org/10.3390/polym14112293>
 22. Al-Zahrani, F.A., et al., Synthesis of Ag/Fe₂O₃ nanocomposite from essential oil of ginger via green method and its bactericidal activity. *Biomass Conversion and Biorefinery*, 2022: p. 1-9. <https://doi.org/10.1007/s13399-022-03248-9>
 23. Gao, N., Y. Chen, and J. Jiang, Ag@Fe₂O₃-GO nanocomposites prepared by a phase transfer method with long-term antibacterial property. *ACS applied materials & interfaces*, 2013. 5(21): p. 11307-11314. <https://doi.org/10.1021/am403538j>
 24. Luengo, Y., B. Sot, and G. Salas, Combining Ag and γ-Fe₂O₃ properties to produce effective antibacterial nanocomposites. *Colloids and Surfaces B: Biointerfaces*, 2020. 194: p. 111178. <https://doi.org/10.1016/j.colsurfb.2020.111178>
 25. Aref, M.S. and S.S. Salem, Bio-callus synthesis of silver nanoparticles, characterization, and antibacterial activities via *Cinnamomum camphora* callus culture. *Biocatalysis and Agricultural Biotechnology*, 2020. 27: p. 101689. <https://doi.org/10.1016/j.bcab.2020.101689>
 26. Khan, A.U., et al., Facile and eco-benign fabrication of Ag/Fe₂O₃ nanocomposite using *Algaia Monozyga* leaves extract and its efficient biocidal and photocatalytic applications. *Photodiagnosis and Photodynamic Therapy*, 2020. 32: p. 101970. <https://doi.org/10.1016/j.pdpdt.2020.101970>
 27. Wei, Z., et al., Multifunctional Ag@Fe₂O₃ yolk-shell nanoparticles for simultaneous capture, kill, and removal of pathogen. *Journal of Materials Chemistry*, 2011. 21(41): p. 16344-16348. <https://doi.org/10.1039/c1jm13691g>
 28. Seddighi, N.S., S. Salari, and A.R. Izadi, Evaluation of antifungal effect of iron-oxide nanoparticles against different *Candida* species. *Iet Nanobiotechnology*, 2017. 11(7): p. 883-888. <https://doi.org/10.1049/iet-nbt.2017.0025>
 29. Nehra, P., et al., Antibacterial and antifungal activity of chitosan coated iron oxide nanoparticles. *British journal of biomedical science*, 2018. 75(1): p. 13-18. <https://doi.org/10.1080/09674845.2017.1347362>
 30. Xie, Y., et al., Antibacterial activity and mechanism of action of zinc oxide nanoparticles against *Campylobacter jejuni*. *Applied and environmental microbiology*, 2011. 77(7): p. 2325-2331. <https://doi.org/10.1128/AEM.02149-10>
 31. Liu, Y.-j., et al., Antibacterial activities of zinc oxide nanoparticles against *Escherichia coli* O157: H7. *Journal of applied microbiology*, 2009. 107(4): p. 1193-1201. <https://doi.org/10.1111/j.1365-2672.2009.04303.x>